

Cation disorder and size effects in magnetoresistive manganese oxide perovskites

Lide M. Rodriguez-Martinez and J. Paul Attfield*

*Department of Chemistry, University of Cambridge, Lensfield Road, Cambridge CB2 1EW, United Kingdom
and Interdisciplinary Research Centre in Superconductivity, University of Cambridge, Madingley Road,
Cambridge CB3 0HE, United Kingdom*

(Received 19 September 1996)

Large disorder effects due to size differences between A -site R^{3+} ($R = \text{La, Pr, Nd, Sm}$) and M^{2+} ($M = \text{Ca, Sr, Ba}$) cations have been found in magnetoresistive $(R_{0.7}M_{0.3})\text{MnO}_3$ perovskites. The ferromagnetic-metal-paramagnetic-insulator transition temperature T_m varies as $T_m = T_m(0) - pQ^2$ due to strain fields resulting from ordered or disordered oxygen displacements Q that are parametrized by the statistical mean and variance of the A cation radius, respectively. The value of p is related to the Mn-O force constant showing that Mn^{3+} Jahn-Teller distortions assist electron localization at T_m . The maximum possible T_m is estimated to be ~ 530 K although experimentally observable values are ≤ 360 K. A large suppression of magnetoresistance due to cation disorder is also evidenced. [S0163-1829(96)51046-5]

The transition between ferromagnetic metallic and paramagnetic insulating states in $(R_{1-x}M_x)\text{MnO}_3$ perovskites is characterized by a maximum in the electrical resistivity ρ_m at the transition temperature T_m . ρ_m decreases greatly in an applied magnetic field B , and this giant negative magnetoresistance (MR) effect¹ may be quantified by the ratio of resistivities in zero and applied fields, $\rho(0)/\rho(B)$, which has a maximum value R_B at a temperature close to T_m . The magnitude of R_B increases greatly as T_m is shifted to lower temperatures, from values of 1–2 at room temperature up to, e.g., $R_{5T} = 250\,000$ in $\text{Pr}_{0.7}\text{Sr}_{0.05}\text{Ca}_{0.25}\text{MnO}_3$ at 85 K.²

The hole-doping x (giving an Mn oxidation state of $3+x$) and the average A -site cation radius $\langle r_A \rangle$ are found to be key chemical variables that control T_m ,^{3–7} giving a maximum $T_m = 360$ K for $x = 0.3$ and $\langle r_A \rangle = 1.23$ Å.⁴ Hole doping in the range $x \approx 0.2$ – 0.5 is needed to stabilize the low-temperature ferromagnetic metallic phase in which a ferromagnetic “double exchange” interaction between the localized t_{2g}^3 electron configurations on adjacent Mn ions is mediated by the itinerant, spin-polarized e_g electrons.⁸ The strong dependence of T_m on $\langle r_A \rangle$ is shown in Fig. 1(a) using experimental values for $(R_{0.7}M_{0.3})\text{MnO}_3$ samples from the literature^{2,4,6,9–11} and this study (Table I). This evidences a very strong coupling of electronic motion to lattice effects in $(R_{1-x}M_x)\text{MnO}_3$ perovskites. Supporting observations include the switching of a lattice distortion in $(\text{La}_{0.83}\text{Sr}_{0.17})\text{MnO}_3$ by an applied magnetic field,¹² striction-coupled MR in the $(\text{Nd, Sm})_{0.5}\text{Sr}_{0.5}\text{MnO}_3$ system,¹³ and a large oxygen isotope effect on the transition temperature in $(\text{La}_{0.7}\text{Ca}_{0.3})\text{MnO}_3$.¹⁴ A further lattice effect whose influence has not been studied in detail, although it is inherent to almost all $(R_{1-x}M_x)\text{MnO}_3$ compositions, is the random disorder of R^{3+} and M^{2+} cations with different sizes distributed over the A sites in the perovskite structure. To quantify this effect, we use the variance (second moment) of the A -cation radius distribution, σ^2 . For two or more A -site species with fractional occupancies y_i ($\sum y_i = 1$), the variance of the ionic radii r_i about the mean $\langle r_A \rangle$ is $\sigma^2 = \sum y_i r_i^2 - \langle r_A \rangle^2$. Standard ionic radii¹⁵ with values 1.216–

1.132 Å for $R^{3+} = \text{La-Sm}$ and 1.18, 1.31, and 1.47 Å for $M^{2+} = \text{Ca, Sr, and Ba}$, respectively, were used to calculate $\langle r_A \rangle$ and σ^2 .

To determine how the properties of $(R_{1-x}M_x)\text{MnO}_3$ perovskites change with the A -site variance σ^2 , we have prepared a series of eight samples (Table I) with fixed doping ($x = 0.3$) and mean A -cation radius ($\langle r_A \rangle = 1.23$ Å), but in which σ^2 is varied by use of different R and M combinations. The samples were prepared under identical conditions by solid-state reaction in air at 1350 °C. Powder x-ray diffraction showed all the samples to consist of a single perovskite phase with the orthorhombic $\sqrt{2}a_p \times 2a_p \times \sqrt{2}a_p$ $Pnma$ superstructure, where a_p is the cubic perovskite cell dimension.¹² The cell parameters a , b , and c were refined by the Rietveld method.¹⁶ Resistivities [Fig. 2(a)] of sintered polycrystalline bars (approximate dimensions $1.5 \times 4 \times 8$ mm³) were measured between 80 and 400 K using a standard four-probe technique and magnetizations M [shown as B/M in Fig. 2(b)] were recorded using a Quantum Design superconducting quantum interference device magnetometer with an applied field $B = 50$ mT. The peak resistivity temperatures T_m are in good agreement with characteristic magnetic transition temperatures T_C defined by minima in dM/dT .⁵

The parameters in Table I all show a strong dependence on σ^2 . The differences between the unit-cell parameters decrease smoothly with increasing σ^2 and the combined effects of disorder and inhomogeneity (discussed below) necessitated tetragonal or cubic cell parameter constraints at high values of σ^2 . T_m shows a strong linear dependence upon σ^2 up to ~ 0.015 Å² (Fig. 3) and then varies around an average value of ~ 100 K above this limit. The latter behavior is due to segregation of the A cations as a result of the large disparities in size, so that the samples are no longer microscopically homogeneous, although they appear to be single phases by powder x-ray diffraction. There is a corresponding change in the low-temperature behavior of the inverse magnetizations [Fig. 2(b)] which, for the three samples with $\sigma^2 > 0.015$ Å², lie substantially above the Curie-Weiss

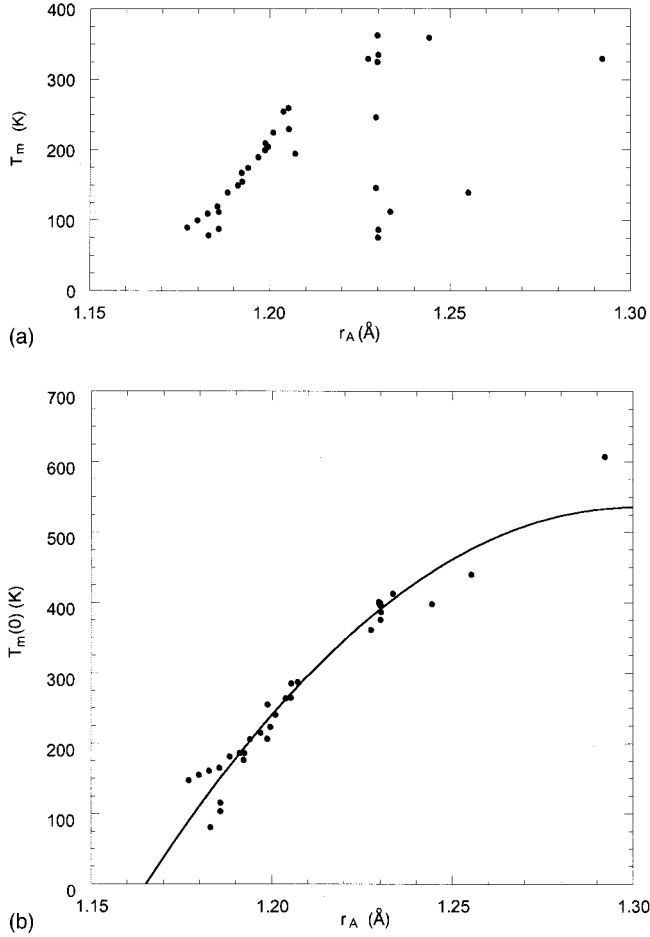


FIG. 1. Plots of (a) experimental T_m values, and (b) $T_m(\sigma^2=0)$ corrected for cation-size disorder using the procedure described in the text, against average A-cation radius for $\text{Ln}_{0.7}\text{M}_{0.3}\text{MnO}_3$ compositions. (b) shows the fit of Eq. (2).

limit as T_C is approached from high temperatures, possibly reflecting a coexistence of antiferromagnetic and ferromagnetic regions.¹⁷ Inhomogeneity is also evidenced by the presence of a second resistive transition in the $\sigma^2=0.0207 \text{ \AA}^2$ sample [Fig. 2(a)], and by the disparity between T_m and

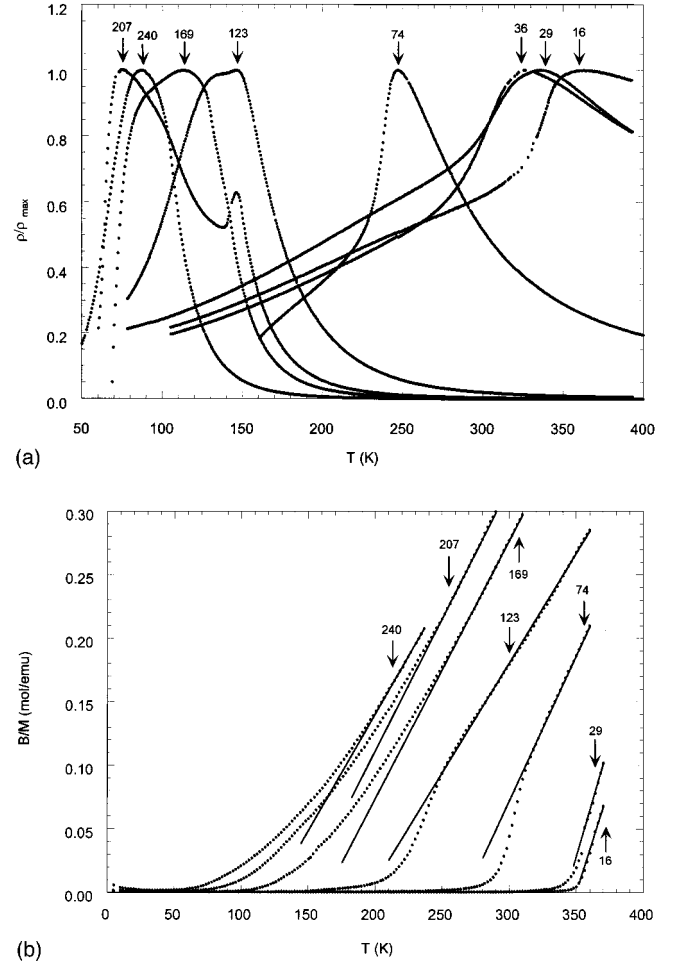


FIG. 2. Plots of (a) normalized resistivity, and (b) inverse magnetization as B/M , with the σ^2 ($\times 10^4 \text{ \AA}^2$) values labeled. The high-temperature Curie-Weiss limits are shown as full lines in (b). Data for the $\sigma^2=0.0036 \text{ \AA}^2$ sample have been omitted from (b) for clarity as they largely overlap the $\sigma^2=0.0029 \text{ \AA}^2$ data.

T_C for the $\sigma^2=0.0240 \text{ \AA}^2$ material (Table I). The nature of the phase segregation will depend upon the sizes of the individual A cations so that T_m is no longer a simple function of σ^2 .

TABLE I. Variation of cell parameters a , b , and c , the resistivity maximum ρ_m , and the metal-insulator transition temperature measured from resistivity (T_m) and magnetization (T_C) data with cation-size variance σ^2 for a series of $(\text{R}_{0.7}\text{M}_{0.3})\text{MnO}_3$ perovskites with constant $\langle r_A \rangle = 1.23 \text{ \AA}$.

A-site composition	σ^2 (\AA^2)	a (\AA)	b (\AA)	c (\AA)	ρ_m ($\Omega \text{ cm}$)	T_m (K)	T_C (K)
$\text{La}_{0.70}\text{Ca}_{0.11}\text{Sr}_{0.19}$	0.0016	5.5045(6)	7.7542(9)	5.4482(6)	1.22×10^{-2}	363	350
$\text{La}_{0.32}\text{Pr}_{0.38}\text{Sr}_{0.30}$	0.0029	5.5046(4)	7.7175(5)	5.4538(3)	1.58×10^{-2}	336	332
$\text{La}_{0.53}\text{Sm}_{0.17}\text{Sr}_{0.30}$	0.0036	5.5089(4)	7.7177(5)	5.4582(3)	1.84×10^{-2}	326	325
$\text{Pr}_{0.70}\text{Sr}_{0.23}\text{Ba}_{0.07}$	0.0074	5.4968(3)	7.7307(4)	5.4700(3)	1.13×10^{-1}	247	248
$\text{Nd}_{0.70}\text{Sr}_{0.16}\text{Ba}_{0.14}$	0.0123	5.4927(3)	7.7345(4)	5.4740(3)	7.96×10^0	146	148
$\text{Nd}_{0.41}\text{Sm}_{0.29}\text{Ba}_{0.20}\text{Sr}_{0.10}$	0.0169	5.4943(3)	7.7328(4)	5.4760(3)	9.94×10^1	87	98
$\text{Nd}_{0.15}\text{Sm}_{0.55}\text{Ba}_{0.25}\text{Sr}_{0.05}$	0.0207	5.4844(4)	7.7484(10)	5.4844 ^a	2.32×10^2	76	72
$\text{Sm}_{0.70}\text{Ba}_{0.30}$	0.0240	5.4879(1)	7.7611 ^b	5.4879 ^b	6.67×10^2	113	60

^a $a=c$ constrained to give stable refinement.

^b $a=b/\sqrt{2}=c$ constrained to give stable refinement.

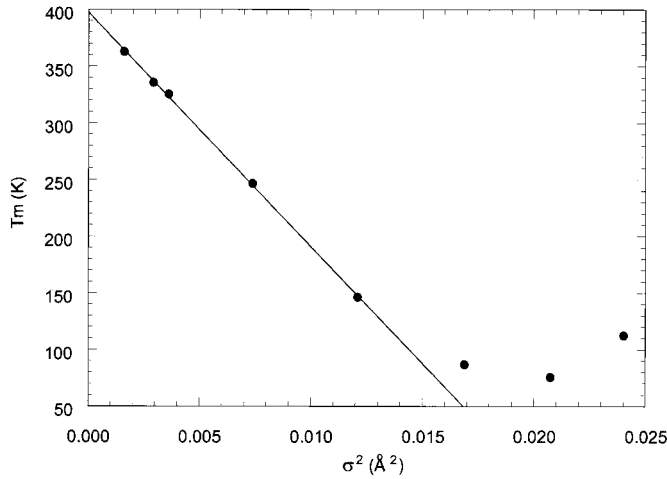


FIG. 3. Variation of T_m with A -cation size variance σ^2 , showing the fit of Eq. (1) to data with $\sigma^2 < 0.015 \text{ \AA}^2$.

A fit to the linear region in Fig. 3,

$$T_m(\langle r_A \rangle, \sigma^2) = T_m(\langle r_A \rangle, 0) - p_1 \sigma^2, \quad (1)$$

gives $T_m(\langle r_A \rangle, 0) = 400 \text{ K}$ and $p_1 = 20\,600 \text{ K \AA}^{-2}$ for our series of samples in which $\langle r_A \rangle = 1.23 \text{ \AA}$. $T_m(\langle r_A \rangle, 0)$ is an estimate of the ideal metal-insulator transition temperature that would be observed if cation-size disorder were not present.¹⁸ Equation (1) has been used to estimate the variation of T_m with $\langle r_A \rangle$ in the absence of cation-size disorder, shown in Fig. 1(b), by extrapolating $T_m(\langle r_A \rangle, 0)$ from T_m for all the reported compositions with $\sigma^2 < 0.015 \text{ \AA}^2$ in Fig. 1(a), assuming the slope p_1 to be independent of $\langle r_A \rangle$. For the small number of samples with $\sigma^2 > 0.015 \text{ \AA}^2$ the cruder approximation $T_m(\langle r_A \rangle, 0) \approx T_m + 300$ based on the inhomogeneous region of Fig. 3 has been used.

A -site cation disorder results mainly in random displacements of oxide ions from their average crystallographic positions. In a close-packed, hard-sphere ionic model of the structure, the mean random displacement is $Q_r \approx \sigma$ ($\sigma = \sqrt{\sigma^2}$ is the standard deviation in the distribution). Changing the mean A -cation radius $\langle r_A \rangle$ results in analogous, ordered oxide displacements for which the mean value is $Q_o \approx r_A^0 - \langle r_A \rangle$, where the ideal radius for an undistorted cubic perovskite is $r_A^0 = 1.30 \text{ \AA}$ for $(R_{0.7}M_{0.3})\text{MnO}_3$ compositions.¹⁹ Hence, following Eq. (1), the disorder-corrected variation of T_m with $\langle r_A \rangle$ should be of the form

$$T_m(\langle r_A \rangle, 0) = T_m(r_A^0, 0) - p_2 (r_A^0 - \langle r_A \rangle)^2, \quad (2)$$

with $p_2 \sim p_1$. This expression is found to give a good fit to the extrapolated data in Fig. 1(b) with refined parameters $T_m(r_A^0, 0) = 530 \pm 20 \text{ K}$ and $p_2 = 29\,000 \pm 1000 \text{ K \AA}^{-2}$. $T_m(r_A^0, 0)$ is an experimental estimate of the metal-insulator transition temperature for an ideal, disorder-free $(R_{0.7}M_{0.3})\text{MnO}_3$ perovskite.

These results show that both the average radius $\langle r_A \rangle$ [Fig. 1(b)] and the size variance σ^2 of the A -site cations (Fig. 3) are key chemical parameters that can be used to tune the metal-insulator transition in $(R_{1-x}M_x)\text{MnO}_3$ perovskites at a constant doping x . In homogeneous samples, the dependence of T_m upon both parameters is described to a good

approximation by equations $T_m = T_m(0) - pQ^2$, where the oxide ion displacements Q in the strain term are random due to A -site disorder [$Q_r \approx \sigma$ in Eq. (1)] or ordered due to the changing average A -cation radius [$Q_o \approx r_A^0 - \langle r_A \rangle$ in Eq. (2)]. The experimental T_m values for $x = 0.3$ [Fig. 1(a)] fall into two regions. For $\langle r_A \rangle < 1.22 \text{ \AA}$, the cation-size variance is small and the true variation of T_m with $\langle r_A \rangle$ is observed. As $\langle r_A \rangle$ increases above 1.22 \AA , the disparity in R and M ($=\text{Sr}$ and Ba) radii gives rise to an increasing σ^2 effect which offsets the increase in $T_m(0)$, resulting in approximately constant T_m values. $\text{La}_{0.7}\text{Ba}_{0.3}\text{MnO}_3$ has the maximum observable $\langle r_A \rangle$ of 1.29 \AA but also a large value of $\sigma^2 = 0.0135 \text{ \AA}^2$ so that T_m is only 320 K although the extrapolated value for an ideal $(R_{0.7}M_{0.3})\text{MnO}_3$ perovskite is $T_m \approx 530 \text{ K}$.

Our results are in agreement with recent mean-field treatments of the metal-insulator transition in $(R_{1-x}M_x)\text{MnO}_3$ perovskites.²⁰ Calculations based upon the double exchange interaction alone give unrealistically high values of $T_m \approx 2500\text{--}5000 \text{ K}$,²¹ but including electron-localizing (polaron) effects due to Jahn-Teller distortions of Mn^{3+}O_6 octahedra gives estimates of $T_m \sim 500 \text{ K}$ for small e_g electron hopping energies $\sim 0.2 \text{ eV}$,²⁰ in agreement with our extrapolated $T_m(r_A^0, 0)$ of 530 K . The Jahn-Teller part of the Hamiltonian contains the lattice strain term $(K/2)\sum Q_b^2$ summed over changes in Mn-O bond lengths Q_b where K is the harmonic force constant for these bonds. Assuming the changes in the T_m to be due principally to this strain energy, then an approximate expression for T_m is

$$T_m(\langle r_A \rangle, \sigma^2) = T_m(r_A^0, 0) - \frac{K}{2\Delta S_m} \sum Q_b^2, \quad (3)$$

where ΔS_m is the entropy change at the transition. If the mean-squared displacements Q^2 ($=Q_r^2$ or Q_o^2) due to changes in the cation variance or average size are assumed to be isotropic then $Q_b^2 = Q^2/3$ and for six Mn-O bonds per cation, Eq. (3) becomes

$$T_m(\langle r_A \rangle, \sigma^2) = T_m(r_A^0, 0) - \frac{KQ^2}{\Delta S_m} \quad (4)$$

so that the experimental coefficients p_1 and p_2 in Eqs. (1) and (2) are $\approx K/\Delta S_m$. Estimating $\Delta S_m \approx k \ln(2\langle S \rangle + 1)$ with $\langle S \rangle = 1.85$ and taking the range of $p \approx 21\,000\text{--}29\,000 \text{ K \AA}^{-2}$ from the experimental fits of Eqs. (1) and (2) gives $K \approx 45\text{--}65 \text{ N m}^{-1}$. This is of the correct magnitude for the Mn-O force constant, given the approximate nature of the calculation, and lies within the range $30\text{--}300 \text{ N m}^{-1}$ estimated for K in LaMnO_3 .²² Hence, the local deformations of the MnO_6 octahedra due to A -cation disorder and size effects act as ‘‘preformed Jahn-Teller distortions’’ that promote the localization of e_g electrons thereby lowering T_m .

Consideration of A -cation size disorder through the variance σ^2 also accounts for variations in MR properties of $(R_{1-x}M_x)\text{MnO}_3$ perovskites with similar T_m values. Negligible disorder ($\sigma^2 < 10^{-6} \text{ \AA}^2$) can be realized in the $\text{Pr}_{1-x}\text{Ca}_x\text{MnO}_3$ system due to the exact size matching of Pr^{3+} and Ca^{2+} , which enables a variety of charge and spin ordered states to be observed.²³ These phases are nonmetallic due to the small $\langle r_A \rangle$ of 1.18 \AA , although a transition to the

ferromagnetic metallic state of $\text{Pr}_{0.7}\text{Ca}_{0.3}\text{MnO}_3$ can be induced by applied pressure,⁶ magnetic fields (resulting in very large MR),^{6,23} or chemical substitutions with La or Sr which increase $\langle r_A \rangle$.^{2,5,24} The latter materials have very high magnetoresistance peaks, up to $R_{5T}=250\,000$ at 85 K in $\text{Pr}_{0.7}\text{Sr}_{0.05}\text{Ca}_{0.25}\text{MnO}_3$.² Phases with comparable $\langle r_A \rangle$ and T_m values, but significant A-cation size disorder, have much smaller MR peaks, e.g., $\text{La}_{0.6}\text{Y}_{0.1}\text{Ca}_{0.3}\text{MnO}_3$ with $\sigma^2=0.0022\text{ \AA}^2$ has R_{5T} of only 40 at 120 K,¹¹ showing that A-cation disorder strongly reduces the magnitude of the magnetoresistive effect. Smaller reductions due to disorder are observed at higher temperatures, e.g., $\text{La}_{0.525}\text{Pr}_{0.175}\text{Ca}_{0.3}\text{MnO}_3$ ($\sigma^2=0.0003\text{ \AA}^2$) has $R_{5T}=10$ at 210 K,⁵ whereas $\text{Nd}_{0.7}\text{Sr}_{0.3}\text{MnO}_3$ ($\sigma^2=0.0044\text{ \AA}^2$) has $R_{6T}=1.5$ at 195 K.⁴

In summary, the metal-insulator transition temperature

and the magnitude of the MR in $(R_{1-x}M_x)\text{MnO}_3$ perovskites are dependent upon the hole-doping x , the mean A-cation radius $\langle r_A \rangle$, and the A-site disorder quantified by the size variance σ^2 . The latter two effects are both described by equations $T_m=T_m(0)-pQ^2$ in which Q is the mean ordered and random oxide ion displacement, respectively, and p is related to the Mn-O force constant. These strain fields reduce T_m considerably from an estimated maximum value of 530 ± 20 K for $x=0.3$ which is in good agreement with recent theoretical estimates. Maximum MR effects are found in materials having a low value of $\langle r_A \rangle$, and hence a low T_m , and a small σ^2 , such as $\text{Pr}_{1-x}\text{Ca}_x\text{MnO}_3$ -based compositions.

The authors acknowledge Dr. S. R. Elliott and Professor E. K. H. Salje for helpful discussions. L.M.R.M. thanks the Basque Government for financial support.

*Author for correspondence. Fax: +44 1223 336362. Electronic address: jpal4@cam.ac.uk

¹R. M. Kusters, J. Singleton, D. A. Keen, R. L. McGreevy, and W. Hayes, *Physica B* **155**, 362 (1989); R. von Helmolt, J. Wecker, B. Holzapfel, L. Schultz, and K. Samwer, *Phys. Rev. Lett.* **71**, 2331 (1993).

²B. Raveau, A. Maignan, and V. Caignaert, *J. Solid State Chem.* **117**, 424 (1995).

³A. Urushibara *et al.*, *Phys. Rev. B* **51**, 14 103 (1995).

⁴R. Mahesh, R. Mahendiran, A. K. Raychaudhuri, and C. N. R. Rao, *J. Solid State Chem.* **120**, 204 (1995).

⁵H. Y. Hwang, S.-W. Cheong, P. G. Radaelli, M. Marezio, and B. Batlogg, *Phys. Rev. Lett.* **74**, 914 (1995).

⁶H. Y. Hwang, T. T. M. Palstra, S.-W. Cheong, and B. Batlogg, *Phys. Rev. B* **52**, 15 046 (1995).

⁷P. G. Radaelli, M. Marezio, H. Y. Hwang, and S.-W. Cheong, *J. Solid State Chem.* **122**, 444 (1996).

⁸C. Zener, *Phys. Rev.* **82**, 403 (1951); P.-G. de Gennes, *ibid.* **118**, 141 (1960).

⁹R. Mahesh, R. Mahendiran, A. K. Raychaudhuri, and C. N. R. Rao, *J. Solid State Chem.* **114**, 297 (1995).

¹⁰S. Jin, H. M. O'Bryan, T. M. Tiefel, M. McCormack, and W. W. Rhodes, *Appl. Phys. Lett.* **66**, 382 (1995).

¹¹A. Maignan, Ch. Simon, V. Caignaert, and B. Raveau, *J. Appl. Phys.* **79**, 7891 (1996).

¹²A. Asamitsu, Y. Moritomo, Y. Tomioka, T. Arima, and Y. Tokura, *Nature (London)* **373**, 407 (1995).

¹³H. Kuwahara *et al.*, *Science* **272**, 80 (1996).

¹⁴G. Zhao, K. Conder, H. Keller, and K. A. Muller, *Nature (London)* **381**, 676 (1996).

¹⁵Ionic radii for ninefold coordination in oxides were taken from R. D. Shannon, *Acta Crystallogr. Sec. A* **32**, 751 (1976).

¹⁶H. M. Rietveld, *J. Appl. Crystallogr.* **2**, 65 (1969).

¹⁷R. Mahendiran *et al.*, *Phys. Rev. B* **53**, 3348 (1996).

¹⁸This extrapolation overestimates $T_m(0)$ slightly as a nonlinear variation of T_m is expected as $\sigma^2 \rightarrow 0$. This "plateau" effect cannot easily be estimated, as a linear variation is observed down to $\sigma^2=0.0016\text{ \AA}^2$ and compositions with smaller variances do not exist in this system. The error due to linear extrapolation is likely to be no more than ~ 10 K. See E. K. H. Salje, *Eur. J. Mineral.* **7**, 791 (1995).

¹⁹ r_A^0 is defined as giving a tolerance factor of $t=1$ for $\langle r_A \rangle=r_A^0$ where $t=(\langle r_A \rangle+r_O)/\sqrt{2}(r_{\text{Mn}}+r_O)$, and r_O and r_{Mn} are the radii of the oxide and manganese ions.

²⁰H. Roder, J. Zang, and A. R. Bishop, *Phys. Rev. Lett.* **76**, 1356 (1996); J. Zang, A. R. Bishop, and H. Roder, *Phys. Rev. B* **53**, R8840 (1996).

²¹A. J. Millis, P. B. Littlewood, and B. I. Shraiman, *Phys. Rev. Lett.* **74**, 5144 (1995).

²²A. J. Millis, *Phys. Rev. B* **53**, 8434 (1996).

²³Y. Tomioka, A. Asamitsu, H. Kuwahara, Y. Moritomo, and Y. Tokura, *Phys. Rev. B* **53**, R1689 (1996).

²⁴A. Maignan, Ch. Simon, V. Caignaert, and B. Raveau, *Solid State Commun.* **96**, 623 (1995).